PHILOSOPHICAL TRANSACTIONS OF THE ROYAL SOCIETY A
MATHEMATICAL, PHYSICAL & ENGINEERING SCIENCES

Turbulent Boundary-Layer Structure in Supersonic Flow

A. J. Smits

Phil. Trans. R. Soc. Lond. A 1991 **336**, 81-93
doi: 10.1098/rsta.1991.0067

Turbulent boundary-layer structure in supersonic flow

By A. J. Smits

Department of Mechanical and Aerospace Engineering, Princeton University, Princeton, New Jersey 08544, U.S.A.

A summary is given of the recent experimental data on the structure of turbulent boundary layers in supersonic flow. The physical mechanisms differentiating incompressible and compressible boundary layers are discussed, and a simple model for the Mach and Reynolds number dependence of the decay of the large-scale motions is proposed.

1. Introduction

When a turbulent boundary layer forms in a supersonic flow, mean density gradients exist in addition to mean velocity gradients, and the turbulent field consists of pressure, density and velocity fluctuations. Energy is continually transferred among these three modes, and the transport mechanisms are therefore more complex than those encountered in constant property flows. In some parts of the flow, the relative speed of adjacent turbulent motions may be transonic or supersonic, and it is possible that local compression waves and 'shocklets' could affect the turbulence evolution. Vorticity can be produced through baroclinic torques, since the density is not just a function of temperature, and energy may be dissipated by sound radiation, in addition to the usual viscous effects.

In some respects, however, the direct effects of compressibility on wall turbulence seem to be rather small, as long as the freestream Mach number is less than about 5. Some of the most notable differences between subsonic and supersonic boundary layers may be attributed to the variation in fluid properties across the layer. As evidence for this assertion, consider the zero pressure gradient boundary layer studied by Spina & Smits (1987), Fernando & Smits (1990), and Spina *et al.* (1990). In this case, the boundary layer developed on the nozzle wall of a blowdown wind tunnel, with a freestream Mach number of about 2.9, and a unit Reynolds number of $69\times10^6\ \mathrm{m}^{-1}$. At the point of interest, the boundary layer thickness was approximately 28 mm, and the Reynolds number based on momentum thickness and freestream conditions was about 80000 (see also table 1). There is a large variation in fluid properties across the layer: the density and viscosity vary by a factor of about three, resulting in a five-fold decrease in kinematic viscosity as we move from the wall to the freestream. The heat transfer is small, typical of supersonic blowdown facilities, so that the wall conditions are nearly adiabatic, and the fluid property variations are caused almost completely by frictional heating.

Now, when the velocity profile is plotted in classic inner (y, u_τ, ν_w) and outer (y, u_τ, δ) layer coordinates, the profile does not follow the log law, as expected. One way to reconcile this is through a modified scaling, taking into account the fluid property variation through the layer. In particular, if the results are normalized by a velocity

Phil. Trans. R. Soc. Lond. A (1991) **336**, 81–93
Printed in Great Britain

4 Vol. 336. A (15 August 1991)

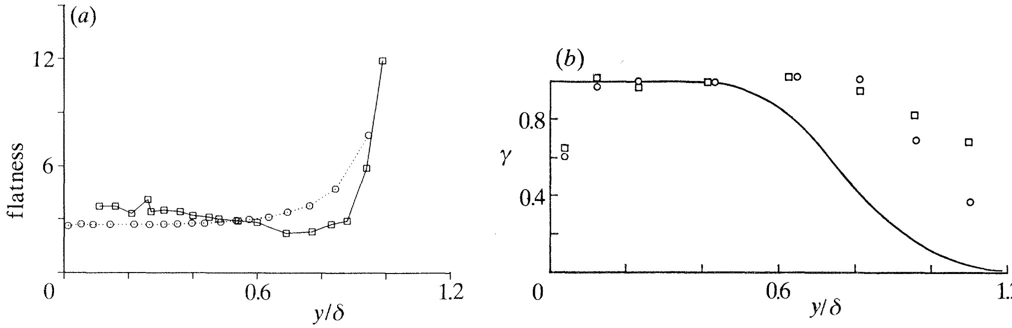

Figure 1. (*a*) Comparison of flatness profiles: □, streamwise mass-flux fluctuations in $M_e = 2.9$ supersonic boundary layer (Spina 1988); ○, streamwise velocity fluctuations in subsonic boundary layer (Alving 1988). Figure from Smits *et al.* (1989). (*b*) Comparison of intermittency distributions: ——, (Klebanoff 1955) $Re_\theta = 7108$, $M = 0.01$; ○, mass flux; □, total temperature (Owen *et al.* 1975), $Re_\theta = 85000$, $M = 7.0$. Figure from Owen *et al.* (1975).

Table 1. *Incoming flow conditions*

$p_0/(\mathrm{Nt\ m^{-2}})$	6.8×10^5
T_0/K	265 ± 5
M_e	2.84 ± 0.04
$U_e/(\mathrm{m\ s^{-1}})$	575 ± 20
$(\rho U)_e/(\mathrm{kg\ m^{-2}\ s^{-1}})$	500 ± 30
Re_e/m	$6.5 \pm 0.5 \times 10^7$
δ/mm	28 ± 1.5
Re_θ	80000
C_f	0.0011 ± 0.0001

scale derived using the wall stress and the local density ($\surd(\tau_w/\rho)$), as suggested by Morkovin (1962), then the velocity profile will collapse on to the 'universal' log-law variation. This rescaling is an example of a compressibility transformation, where it is assumed that by adopting scales which take into account the fluid property variations, the profiles can be made to collapse on to incompressible correlations. The success of such transformations suggests that the intrinsic effects of compressibility are small, and that it is sufficient to treat the compressible high-speed boundary layer as a flow with non-uniform fluid properties, that is, the density (or temperature) variation does not affect the dynamics of the flow, but simply acts as a passive 'stratification', bearing in mind that buoyancy effects are always negligible in high-speed flows.

What about the turbulence? The simplest comparison between the turbulence behaviour in subsonic and supersonic boundary layers is to compare the distributions of $\langle u' \rangle$ ($= \sqrt{\overline{u'^2}}$, where u' is the instantaneous value of the longitudinal velocity fluctuation). When normalized by u_τ ($= \surd(\tau_w/\rho_w)$), the distributions appear to show a strong Mach number effect (see, for example, Schlichting 1968, p. 659), but if the velocity scale is $\surd(\tau_w/\rho)$, the Mach number dependence is no longer evident (see Smits *et al.* (1989) for further discussion).

In contrast, a more detailed inspection of the turbulence properties reveals certain characteristics that cannot be collapsed by a simple density scaling. For example, it is well known that the intermittency profile is fuller than the corresponding subsonic profile (see, for example, Owen *et al.* 1975; Robinson 1986; Smits *et al.* 1989). One definition of intermittency is $I = (3/\text{flatness})$, where flatness $= \overline{u'^4}/(\overline{u'^2})^2$. The results

PHILOSOPHICAL TRANSACTIONS OF THE ROYAL SOCIETY A MATHEMATICAL, PHYSICAL & ENGINEERING SCIENCES

(a)

(b)

(c)

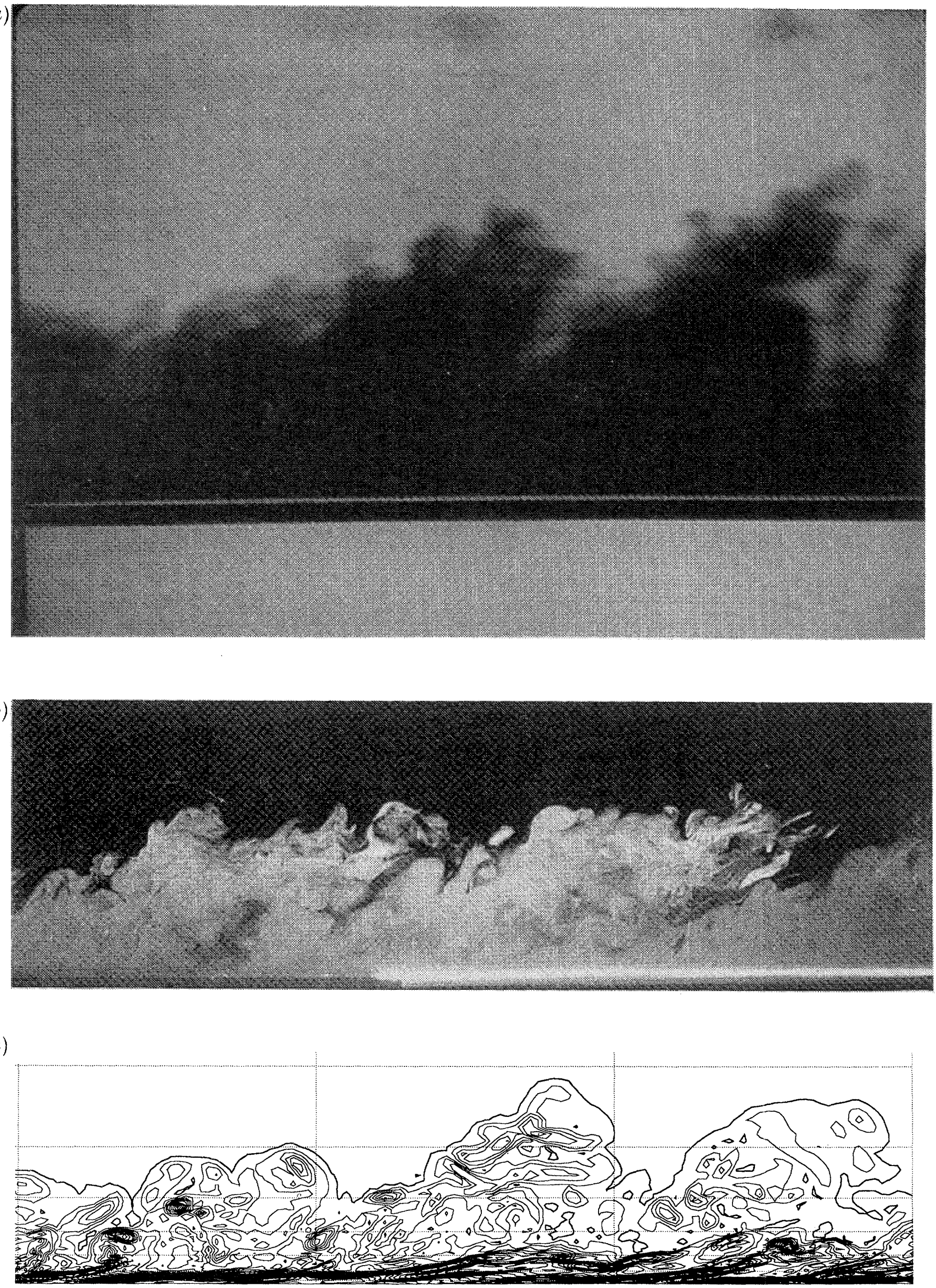

Figure 2. (*a*) Streamwise cross-section of a Mach 2.5 boundary layer with $Re_\theta = 25000$, obtained using Rayleigh scattering; Smith *et al*. (1988). (*b*) Streamwise cross-section of a subsonic boundary layer with $Re_\theta = 4000$, obtained using oil droplet visualization (Falco 1977). (*c*) Streamwise cross-section of a computer-generated subsonic boundary layer with $Re_\theta = 670$, showing iso-vorticity contours. The flow is direct Navier–Stokes simulation (Spalart 1988; Robinson 1990). Figure from Spina *et al*. (1991).

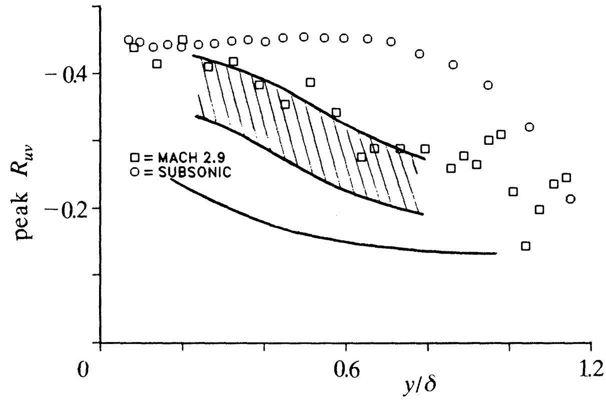

Figure 3. Comparison of the shear correlation coefficient: □, $M_e = 2.9$ supersonic boundary layer (Spina 1988); ○, subsonic boundary layer (Alving 1988); ——, computation (Dussauge & Quine 1988). The hatched area indicates the best estimate for the supersonic data from an error analysis of the systematic and random errors.

for the flatness factors obtained by Spina (1988) are given in figure 1*a*, and they show a distribution significantly different from similar subsonic data, such as that taken by Alving *et al.* (1990). Corresponding values of the intermittency factor are shown in figure 1*b*.

Recently, Smith (1989) and Smith *et al.* (1990*a*) used Rayleigh scattering to visualize the instantaneous density field in supersonic boundary layers at Mach numbers of 2.5 and 2.9 respectively. An example of an image showing a cross-section of the boundary layer in a plane parallel to the wall is given in figure 2 (note the superficial similarity with cross-sections of incompressible boundary layers). These and similar data were used by K. R. Sreenivasan and A. Johnson (personal communication), and J. Poggie (personal communication) to estimate the fractal dimension of the density interface, and the results indicated a decrease with Mach number, where a representative value for the supersonic case was 1.2, compared with a typical value for a subsonic boundary layer of 1.35. This observation may be interpreted as a decrease in mixing across the turbulent–non-turbulent interface, and seems to support the conclusion of a reduced level of intermittency with increasing Mach number.

The skewness ($\overline{u'^3}/(\overline{u'^2})^{\frac{3}{2}}$) also shows significant differences, and what is even more interesting is that the shear correlation coefficient R_{uv} ($=\overline{u'v'}/\langle u'\rangle\langle v'\rangle$) is different (Smits *et al.* 1989). The subsonic data reveal a higher correlation across the boundary layer with a nearly constant value of 0.45 for $0 < y/\delta < 0.8$, while the supersonic correlation decreases steadily as y/δ increases (see figure 3).

In addition, Smits *et al.* (1989) found that the length scales derived from space-time correlations indicate that the spanwise scales were almost identical but that the streamwise scales in Alving *et al.*'s (1990) subsonic flow were about half the size of those in the supersonic flow. The large-scale structures in the subsonic boundary layer also appear to lean more toward the wall than those observed in supersonic flows, and their shear stress content is distributed differently among the four quadrants. On the other hand, Spina *et al.* (1990) indicate that the convection velocity distribution of the large-scale motions appears to be 'universal', independent of Mach and Reynolds number. Furthermore, Spina *et al.* (1991) found that the

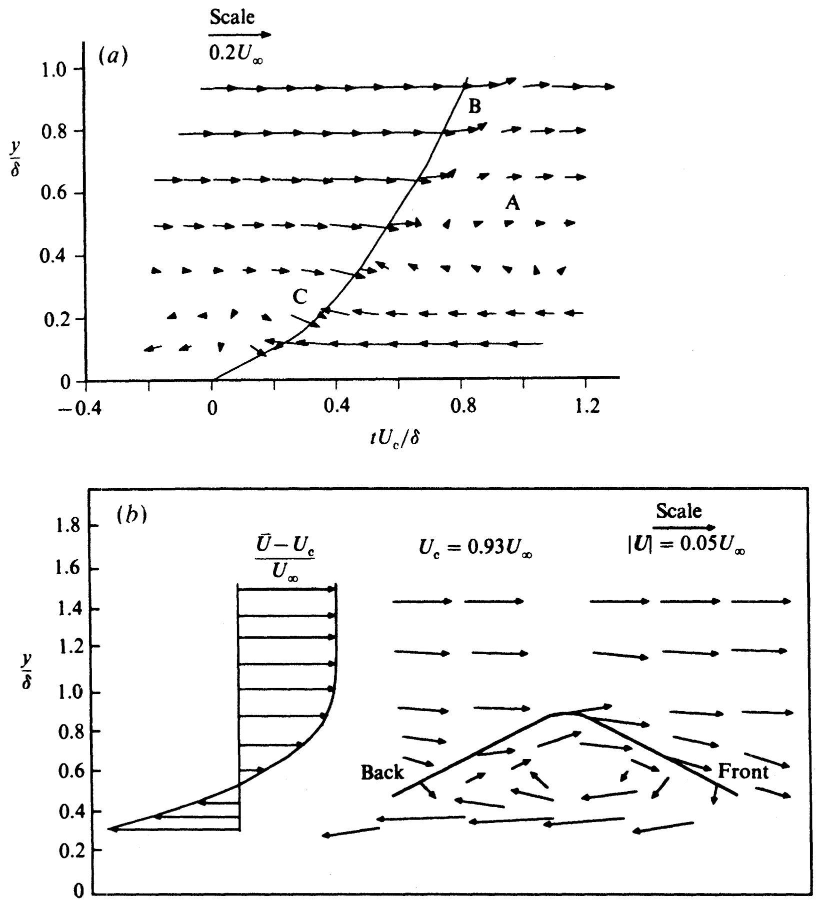

Figure 4. (*a*) Ensemble-averaged flow field upstream and downstream of +VITA events, in a reference frame moving with the convection velocity of the large-scale motions. $M_e = 2.9$ supersonic boundary layer (Spina *et al.* 1991). (*b*) Schematic of a large-scale turbulent 'bulge' in incompressible flow (Blackwelder & Kovasznay 1972). Figure from Spina *et al.* (1991).

Table 2. *Calculated and measured decay distances for large-scale motions* (*Smith & Smits 1991*)

	Re_δ	M	y/δ	y^+	$x_{0.5}/\delta$	x_d/δ	$x_{0.5}/x_d$
Favre *et al.*	27900	0.04	0.03	34	0.65	9	0.07
			0.15	170	2.0	10	0.21
			0.77	872	7	13	0.55
Kovasznay *et al.*	27500	0.14	0.5	617	5.0	10	0.48
Owen & Horstman	218300	7.2	0.08	80	9	31	0.29
			0.15	150	21	45	0.47
			0.3	300	27	71	0.38
Klebanoff	73114	0.05	0.75	2070	—	22	—

ensemble-averaged flowfield associated with the outer-layer bulges was very similar to that observed by, for example, Blackwelder & Kovasznay in incompressible flow (see figure 4).

Finally, there is an order-of-magnitude decrease in the rate of decay of the large-scale motions seen between low subsonic and high supersonic flows. Consider the measurements of the longitudinal space-time correlations for optimum time delay by Favre *et al.* (1957, 1958) and Owen & Horstman (1972). Denoting the longitudinal distance in the point where the correlation falls to a level of 0.5 by the symbol $x_{0.5}$, we see that at $y/\delta = 0.15$ the supersonic data gives a value ten times larger than the subsonic data (see table 2).

2. Physical considerations

How can we explain these differences? Most of our understanding of turbulent boundary-layer structure is based on studies of 'canonical' boundary layers, that is, boundary layers developing on a flat plate, in a zero pressure gradient, with an adiabatic wall, under incompressible flow conditions. In addition, most studies have usually been performed at low Mach numbers, so that the inner layer occupies a significant fraction of the total boundary layer, and laboratory measurements could be obtained with sufficient resolution. It seems doubtful that models for boundary-layer structure derived from such studies can be applied to a wider range of flow conditions. In particular, how can the effects of Mach and Reynolds number be incorporated?

Clearly, at positions in the layer close to the wall, in the viscous sublayer and buffer regions, Reynolds number effects will always be important. In the outer layer, however, it has been widely held that Reynolds number effects are important only at 'low' Reynolds numbers, where a commonly quoted cut-off value for low Reynolds numbers is taken to be where the Reynolds number, based on a momentum thickness, exceeds a value of 5000. This value corresponds to where the wake factor of the mean velocity profile appears to become Reynolds number-independent (see, for example, Coles 1962).

In supersonic flow, where there is usually a significant Mach number gradient across the boundary layer, fluid property variations cause the Reynolds number to vary across the layer, and a single Reynolds number cannot be used to characterize the state of the boundary layer. For example, for the flow given in table 1, the momentum thickness Reynolds number decreases from about 80000 to 15000 if the fluid properties are evaluated at the wall temperature rather than the freestream temperature. To illustrate this another way, we see from table 2 that the Reynolds number based on boundary-layer thickness is about eight times larger for the high Mach number flow of Owen & Horstman (1972) than it is for the low subsonic flow studied by Favre *et al.* Yet in terms of wall units the thicknesses of the two layers are almost identical.

So we expect in a turbulent boundary layer at high speeds that the outer layer is not going to behave too much differently from the incompressible case, in that Mach number gradients are small, so that the turbulent motions are at low subsonic speeds relative to each other and compressibility effects are small, and that fluid property variations are small so that the Reynolds number is relatively constant. Morkovin's (1962) strong Reynolds analogy is expected to hold, where

$$T'/T = -(\gamma-1)M^2 u'/U,$$

although there clearly exists an upper limit, to avoid an unphysically large increase in temperature fluctuations T' as the Mach number increases (see Gaviglio (1987) and Spina *et al.* (1991) for a more complete discussion).

In the inner layer conditions are quite different. The Mach number gradient and the fluid property gradients have their maximum values in this region, as do the levels of turbulent activity. It seems reasonable to expect that relative speeds of the turbulent motions will become transonic, and eventually supersonic, as the freestream Mach number increases. Taking the maximum root mean square (r.m.s.) level of velocity fluctuation found near the wall, and forming a turbulent Mach number m ($= \langle u' \rangle / a$), indicates that m must approach one with a freestream Mach number of about 5. Compressibility effects will therefore become dynamically important somewhere near a Mach number of 5 (for adiabatic walls). This Mach number is also the commonly accepted lower limit for the onset of hypersonic flow. At the same time, large changes in density and viscosity exist, which are strongly dependent on heat transfer, and therefore the thickness of the sublayer will depend on Mach number, Reynolds number, and wall temperature.

These considerations give rise to many questions, for which we do not have any satisfactory answers. At what Mach and Reynolds number does the pressure–velocity term begin to affect the flow dynamics? It appears from the work of Fernholz & Finley (1980), using the data of Watson *et al.* (1973), that Morkovin's density-dependent velocity scale satisfactorily collapses the mean velocity data in zero pressure gradient flows at Mach numbers up to at least 10. But when will shocklets and sound radiation play a significant role in altering the turbulence structure? What is the coupling between the instantaneous density and velocity fields? In other words, to what extent does the strong Reynolds analogy hold? At Mach 2.9, the correlation between u' and T' appears to be almost perfect, even instantaneously (Smith & Smits 1990), but no data are available at higher Mach numbers. The answers to these questions are important if we are to predict practical flows with strong pressure gradients with some degree of confidence. Unfortunately, reliable turbulence data at high Mach numbers are rare in number, and some data simply do not exist. For instance, correlation measurements of any kind are not available above Mach 7, and therefore at the present time little can be said about the structure of high Mach number flows.

What about near-wall phenomena? How does the viscous instability of the sublayer change when fluid properties vary with distance from the wall? Do fluid property variations just change the effective Reynolds number? Since the Reynolds number increases away from an adiabatic wall faster than in an incompressible flow (as the temperature decreases away from the wall, the viscosity decreases and the density increases, causing the kinematic viscosity to decrease rapidly), then we would expect the flow to become less stable as we move away from the wall at a rate which is faster than in an incompressible flow at the same friction velocity. What is the proper basis of comparison between compressible and incompressible boundary layers in the near wall region? And in the outer region? Given that the kinematic viscosity changes dramatically across the layer, how do the dissipation rates vary?

Now, compressibility and fluid property variations are expected to play some role in the inner layer, and a negligible role in the outer layer. But the fact that the outer layer turbulence displays a sensitivity to Mach number gives some evidence for the interaction between the inner and outer layer motions. The process is still very poorly understood and remains the subject of controversy, but it may be possible that the study of high-speed boundary layers can contribute to a deeper understanding of this interaction.

PHILOSOPHICAL TRANSACTIONS OF THE ROYAL SOCIETY A MATHEMATICAL, PHYSICAL & ENGINEERING SCIENCES

3. The role of pressure fluctuations

At supersonic speeds, it is generally supposed that pressure fluctuations are small enough to be neglected. At Mach 2.3, for example, the r.m.s. wall pressure fluctuation level is of the order of 1–2%, and the freestream level is less than half that value (Dolling & Dussauge 1989). Dussauge *et al.* (1989) noted that the contribution of the pressure fluctuations to the divergence of the fluctuating velocity div (u') is small, as long as $m \ll 1$. Under these conditions, div (u') itself is small, and the fluctuating field is nearly solenoidal. Now, in many flows $m \ll 1$, but the density fluctuations are not small. Then the velocity field is solenoidal but the turbulent diffusion of momentum and kinetic energy, for example, and the return to isotropy can be modified by the density fluctuations (Dussauge & Quine 1989).

To identify the role of the pressure fluctuations more clearly, Brown & Roshko (1974) compared the governing equations for two-dimensional supersonic and incompressible, variable-density, plane turbulent mixing layers. The mean continuity and momentum equations for these two cases are identical, but the additional equation to be satisfied for the supersonic flow is the energy equation:

$$P[\partial U/\partial x + \partial V/\partial y] + \partial(\overline{p'v'})/\partial y + \gamma^{-1} V\, \partial p/\partial y = 0, \tag{1}$$

whereas for the incompressible flow it is the diffusion equation that needs to be satisfied. To the boundary-layer approximation the two equations are identical only if $(1/P)\,\partial(\overline{p'v'})/\partial y$ is negligible compared with div U. In other words, the pressure–velocity correlation can be used to characterize the significance of compressibility effects distinct from any intrinsic density effects. An order of magnitude analysis suggests that

$$\alpha \Delta U_s + V_s + U_s\, \alpha^3 M^2 + V_s\, \alpha^2 M^2 = 0, \tag{2}$$

where U_s and V_s are the velocity scales, and L and δ are the length scales for the x and y directions respectively. The parameter $\alpha = \delta/l$. Thus the magnitude of the contribution of the pressure–velocity correlation term, relative to the other terms, depends on the non-dimensional parameter $C = \alpha^2 M^2$. The parameter C is evidently a function of Reynolds number and Mach number, and this analysis suggests that the dynamic importance of the pressure velocity correlation decreases (slowly) with increasing Reynolds number, and increases quadratically with Mach number.

As Dussauge & Quine (1989) pointed out, the pressure–strain terms in the Reynolds stress equations should also include the effects of density fluctuations, and they proposed a modification to Rotta's model of the return-to-isotropy to take this into account. Calculations using a second-order closure predicted that the shear correlation coefficient is a decreasing function of the Mach number, in agreement with the limited experimental evidence available (see figure 3).

4. Mach and Reynolds number effects on structure

As suggested earlier, some of the models based on observations in low Reynolds number, incompressible flows do not extrapolate well to other flow conditions. For example, the visualization of Falco (1977) at a Re_θ of 4000 showed the presence of two outer layer scales, large-scale turbulent bulges and smaller 'typical eddies' which appear on the backs of the bulges (figure 2*b*). Falco measured the size of the typical eddies to be 200 and 100 wall units in the streamwise and vertical directions respectively, and found these sizes to be independent of Reynolds number over the range $1000 < Re_\theta < 10000$. If the typical eddies truly scale on wall variables, then as Reynolds number increases they will decrease in size relative to the largest scale bulges. At high enough Reynolds numbers the typical eddy scaling separates them so far in frequency space from the energetic motions in the outer layer (which remain bounded at frequencies below about $10U_e/\delta$) that they are unlikely to be dynamically significant away from the wall, that is, carry a significant amount of shear stress.

One study that attempts to illustrate qualitatively the effects of Reynolds number on the large structure of the outer layer is Head & Bandyopadhyay (1981). Their flow visualization results show the dramatic effect of increasing Reynolds number on the structure of the boundary layer. They propose that the whole of the boundary layer (inner and outer layers) is populated by vortex loops which have a low aspect ratio and appear as horseshoes at $Re_\theta = 600$. As the Reynolds number increases, these loops are elongated until they appear as 'hairpins' at $Re_\theta = 10000$. In this model, the outer layer bulges are made up of a large number of hairpins, which act largely as a single structure, and Falco's typical eddies are the heads of hairpin eddies. With increasing Reynolds number, it seems reasonable to expect further groupings of hairpins to occur, giving rise to a hierarchy of larger scale motions, as long as the hairpin structure continues to be an important element of high Reynolds number turbulence (see Smits *et al.* (1989) for additional discussion).

5. A hypothesis for the decay of the large-scale motions

To understand the dynamics of these hairpin structures, it is useful to consider the behaviour of a stretching vortex in a viscous fluid: if the hairpins originate near the wall, grow by stretching, and die by viscous cancellation of vorticity (see Smith *et al.* 1990*b*), the solution to this model problem may indicate whether hairpin eddies are a suitable prototype for high Reynolds number large-scale motions.

A line vortex in a viscous fluid has a representative scale r_0, given by the location of maximum tangential velocity. The rate of change of this radius will depend on two competing influences: its rate of increase due to viscous diffusion, and its rate of decrease due to stretching. Hence:

$$\mathrm{d}r_0^2/\mathrm{d}t = 2\nu - (r_0^2/x)\,\mathrm{d}x/\mathrm{d}t, \tag{3}$$

which has the general solution

$$\frac{r_0^2}{r_0^2(0)} = \frac{1}{x}\left(x_0 + \frac{2\nu}{r_0^2(0)}\int_0^t x\,\mathrm{d}t\right), \tag{4}$$

where x is the length of a piece of the vortex at time t, ν is the local kinematic viscosity, and $r_0(0)$ and x_0 are respectively the radius and length of the same piece of the vortex at time $t = 0$. For a stretching given by

$$\mathrm{d}x/\mathrm{d}t = U(x/x_0)^a \tag{5}$$

we have, for $a = 1$,

$$r_0^2/r_0^2(0) = b^{-1}[1 + A(b^{2-a} - 1)] \tag{6}$$

at the time when the length x_0 has grown to become bx_0 $(b > 1)$. Here,

$$A = 2\nu x_0/(2-a)\,Ur_0^2(0). \tag{7}$$

The case of exponential stretching ($a = 1$) was considered previously by Batchelor

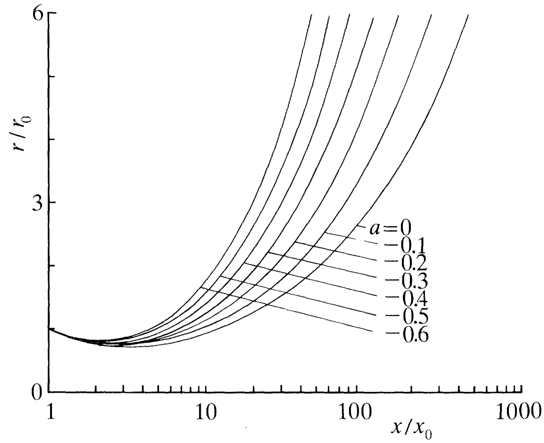

Figure 5. Calculations for the stretching of a rectilinear vortex in a viscous fluid ($A = 0.075$).

(1970), and that of linear stretching by Perry & Chong (1982). The present solution allows a much wider range of stretching rates to be considered. The parameter A may be estimated by adopting some approximate values appropriate to hairpins, that is: $x_0 = 50\nu/u_\tau$, $r_0 = 10\nu/u_\tau$, $U = U_e - U_c = 0.2U_e$ and $C_f = 0.004$, which gives $A = 0.1$. To illustrate some of the implications, the solution for $A = 0.075$ is given in figure 5. Note that for all stretching rates at this value of A the radius of the vortex first decreases because stretching dominates over diffusion, and then increases as the situation is reversed.

Such calculations indicate that high aspect ratio hairpin vortices can develop, even with modest stretching rates (that is, rates considerably less than linear rates). If a five-fold increase in radius is taken to be the cut-off at which viscous diffusion has acted to cancel the vorticity contained in the two legs of the hairpin (which have opposite signs of vorticity), then even with $a = 0.5$ an aspect ratio of 200 seems possible, corresponding to a boundary layer thickness (in incompressible flow) of the order of 20000 wall units, and a Reynolds number based on momentum thickness of about 70000.

Clearly, the rate of stretching of the hairpin depends on the proximity of the wall and therefore the local level of shear. In its early phase of growth, when it is confined to the near-wall region and its aspect ratio is of order one, the presence of high gradients in the surrounding velocity field suggest a rapid stretching. In its late phase, where the hairpin has grown to ‘fill’ the boundary layer, its rate of stretching in the outer flow is of the order of the boundary layer growth, which at high Reynolds number is rather slow.

If we restrict ourselves to considering the outer layer motions, and we assume that they are made up of a large number of hairpins undergoing a negligible stretching, we can now suggest a hypothesis which accounts for the effect of Reynolds number and Mach number on the average streamwise scale of the large-scale outer layer structures (further details are given by Smith & Smits 1991). We assume that the outer layer bulges convect downstream with a constant convection velocity, U_c. Let us suppose that the spanwise spacing of the counter-rotating legs of the hairpins is set by the near-wall streak spacing, equal to an average value of $100\nu_w/u_\tau$ (see Kline *et al.* 1967). Then, if a hairpin is assumed to ‘die’ due to the cancellation of vorticity by viscous diffusion, at a rate set by the *local* kinematic viscosity, it is possible to

PHILOSOPHICAL TRANSACTIONS OF THE ROYAL SOCIETY A MATHEMATICAL, PHYSICAL & ENGINEERING SCIENCES

write a simple expression for the lifetime, t_{d}, of a hairpin vortex. If we take the diffusion distance to be, say, one quarter the average streak spacing, we obtain

$$\surd(\nu t_{\mathrm{d}}) = 25\nu_{\mathrm{w}}/u_{\tau}, \tag{8}$$

where the subscript w refers to the conditions at the wall, and the subscript e to the conditions in the freestream (these distinctions are important when considering a compressible flow). During the time t_{d}, the hairpin will convect downstream a distance, x_{d}, given by $x_{\mathrm{d}} = U_{\mathrm{c}}\, t_{\mathrm{d}}$. Thus,

$$\surd(\nu x_{\mathrm{d}}/u_{\mathrm{c}}) = 25\nu_{\mathrm{w}}/u_{\tau}. \tag{9}$$

Hence,

$$\frac{x_{\mathrm{d}}}{\delta} = \frac{625}{C_{\mathrm{f}}\, Re_{\delta}}\left(\frac{\mu_{\mathrm{w}}}{\mu_{\mathrm{e}}}\right)^{2} \frac{\rho_{\mathrm{e}}}{\rho_{\mathrm{w}}} \frac{U_{\mathrm{c}}}{U_{\mathrm{e}}} \frac{\nu_{\mathrm{e}}}{\nu}. \tag{10}$$

Now, assuming that fluid properties vary according to

$$\mu_{\mathrm{w}}/\mu_{\mathrm{e}} = (T_{\mathrm{w}}/T_{\mathrm{e}})^{0.75}, \quad \rho_{\mathrm{e}}/\rho_{\mathrm{w}} = T_{\mathrm{w}}/T_{\mathrm{e}},$$

we obtain

$$\frac{x_{\mathrm{d}}}{\delta} = \frac{1250}{C_{\mathrm{f}}\, Re_{\delta}}\left(\frac{T_{\mathrm{w}}}{T_{\mathrm{e}}}\right)^{2.5} \frac{U_{\mathrm{c}}}{U_{\mathrm{e}}} \frac{T_{\mathrm{e}}}{T}. \tag{11}$$

Experimentally, the average rate of decay of the large-scale motions can be obtained from streamwise space-time correlations, and such data are given by Favre *et al.* (1957, 1958), Kovasznay *et al.* (1970) and Owen & Horstman (1972). The details of each experiment, and the calculated values of x_{d} are given in table 2. It may be seen that for these two widely different flows, the distance at which the peak in the space-time correlation falls to 0.5 ($= x_{0.5}$) correlates well with x_{d}, at least for $y^{+} > 80$.

The reduced rate of dissipation at higher Mach numbers suggests a correspondingly lower level of shear stress, and therefore this simple model may help to understand (in addition to the role of the pressure–velocity correlation) why the shear correlation coefficient in the outer layer is reduced below the subsonic value (figure 3).

Furthermore, if the rate of formation of the hairpin loops remains unaffected by their rate of decay, then the slower the decay of the outer layer structures, the lower the intermittency levels in the outer layer. The results of our hypothesis appear to be in accord with the experimental results. For example, the values of x_{d} calculated for the Owen *et al.* (1975) and Klebanoff (1955) experiments show the same trend as the intermittency levels obtained in these experiments (see figure 2).

The model proposed here has some interesting features.

First, it assumes that viscosity plays an important role in setting the timescales of the outer layer motions, contrary to popular opinion, which holds that in the fully turbulent part of the boundary-layer viscosity only serves to dissipate energy without influencing the scaling. However, this conclusion has mostly been based on experience with constant property flows where viscous-dependent effects may not be strongly evident. It is interesting to note that the analysis by Fernholz & Finley (1980) of a large sample of supersonic mean flow data indicated that a better length scale for the outer layer is actually a modified Clauser or Rotta thickness ($= \delta\surd(2/C_{\mathrm{f}})$), rather than the boundary-layer thickness, suggesting a viscous dependence of the outer layer. There is also the largely unresolved question of the interaction between the inner and outer layer. Some degree of interaction is entirely to be expected (see, for example, Walker (1990) for a compelling argument), and therefore the outer layer motions must show some level of dependence on viscosity.

Secondly, the model is unlikely to hold at higher Mach numbers (greater than 7), where energy transfer and dissipation due to pressure fluctuations and 'true' compressibility effects are expected to become important. That it even seems to hold at a Mach number of 7 could be taken as support for the observation that the influence of compressibility (such as that caused by pressure fluctuations) on wall bounded flows at supersonic Mach numbers appears to be rather weak.

Thirdly, the model supposes that hairpin vortices of high aspect ratio persist as a dynamical feature of the outer flow for very long times, especially in flows where there is a large decrease in the viscosity away from the wall, as in hypersonic flows. It follows that transition effects, for example, will be felt for a long distance downstream, especially in hypersonic flows. This has been a concern in the hypersonic community for some time, and the present model may serve as a guide for designing turbulent hypersonic boundary layer experiments.

Fourthly, for a hairpin vortex to achieve a high aspect ratio in the first place requires that vortex stretching must dominate viscous diffusion during its growth. Considerations of a stretching, viscous vortex (presented earlier) indicates that the stretching rate must be Reynolds number dependent, which appears to be consistent with the evolution of the outer-layer velocity distribution as a function of Reynolds number.

This work was conducted under AFOSR Grants 90-0217 and 89-0420, monitored by Dr J. McMichael.

References

Alving, A. E. 1988 Boundary layer relaxation from convex curvature. Ph.D. thesis, Princeton University, U.S.A.

Alving, A. E., Smits, A. J. & Watmuff, J. H. 1990 Turbulent boundary layer relaxation from convex curvature. *J. Fluid Mech.* **211**, 529–556.

Batchelor, G. K. 1970 *An introduction to fluid dynamics*. Cambridge University Press.

Brown, G. L. & Roshko, A. 1974 On density effects and large structure in turbulent mixing layers. *J. Fluid Mech.* **64**, 775.

Coles, D. E. 1962 The turbulent boundary layer in a compressible fluid. *RAND Corp. Rep.* R-403-PR.

Dolling, D. S. & Dussauge, J.-P. 1989 Fluctuating wall-pressure measurements. In *AGARDograph* 315.

Dussauge, J.-P. & Quine, C. 1989 A second-order closure for supersonic turbulent flows – application to the supersonic mixing. In *Proc. Symp. Physics of Compressible Turbulent Mixing*. New York: Springer.

Dussauge, J.-P., Debieve, J.-F. & Smits, A. J. 1989 Rapidly distorted compressible boundary-layers. In *AGARDograph* 315.

Falco, R. E. 1977 Coherent motions in the outer region of turbulent boundary layers. *Phys. Fluids* **20**, S124.

Favre, A. J., Gaviglio, J. J. & Dumas, R. 1957 Space-time double correlations and spectra in a turbulent boundary layer. *J. Fluid Mech.* **2**, 313.

Favre, A. J., Gaviglio, J. J. & Dumas, R. 1958 Further space-time correlations of velocity in a turbulent boundary layer. *J. Fluid Mech.* **3**, 344.

Fernando, E. M. & Smits, A. J. 1990 A supersonic turbulent boundary layer in an adverse pressure gradient. *J. Fluid Mech.* **211**, 285–307.

Fernholz, H. & Finley, P. J. 1980 A critical commentary on mean flow data for two-dimensional compressible turbulent boundary layers. In *AGARDograph* 253.

Gaviglio, J. 1987 Reynolds analogies and experimental study of heat transfer in the supersonic boundary layer. *Int. J. heat Mass Transfer* **30**, 911.

Head, M. R. & Bandyopadhyay, P. B. 1981 New aspects of turbulent boundary layer structure. *J. Fluid Mech.* **107**, 297.

Klebanoff, P. S. 1955 Characteristics of turbulence in a boundary layer with zero pressure gradient. *NACA Rept. 1247*.

Kline, S. J., Reynolds, W. C., Schraub, F. A. & Runstadler, P. W. 1967 The structure of turbulent boundary layers. *J. Fluid Mech.* **30**, 741.

Kovasznay, L. S. G., Kibens, V. & Blackwelder, R. F. 1970 Large-scale motion in the intermittent region of a turbulent boundary layer. *J. Fluid Mech.* **41**, 283.

Morkovin, M. V. 1962 Effects of compressibility on turbulent flows. In *Proc. Int. Symp. Mechanique de la Turbulence* (ed. A. J. Favre), pp. 367–380. Paris: Centre National de la Recherche Scientifique.

Owen, F. K. & Horstman, C. C. 1972 On the structure of hypersonic turbulent boundary layers. *J. Fluid Mech.* **53**, 611.

Owen, F. K., Horstman, C. C. & Kussoy, M. I. 1975 Mean and fluctuating flow measurements of a fully developed, non-adiabatic hypersonic boundary layer. *J. Fluid Mech.* **70**, 393.

Perry, A. E. & Chong, M. S. 1982 On the mechanism of wall turbulence. *J. Fluid Mech.* **119**, 173–217.

Robinson, S. K. 1986 Space-time correlation measurements in a compressible turbulent boundary layer. *AIAA Paper* 86-1130.

Robinson, S. K. 1990 A review of vortex structures and associated coherent motions in turbulent boundary layers. In *Structure of turbulence and drag reduction* (ed. A. Gyr). Springer-Verlag.

Schlichting, H. 1968 *Boundary layer theory*, 6th edn, p. 659. New York: McGraw-Hill.

Smith, C. R., Walker, J. D. A., Haidari, A. H. & Taylor, B. K. 1990*a* Hairpin vortices in turbulent boundary layers: the applications for reducing surface drag. In *Structure of turbulence and drag reduction* (ed. A. Gyr). Springer-Verlag.

Smith, D. R. & Smits, A. J. 1990 Velocity and temperature measurements in a Mach 3 turbulent boundary layer. In *Proc. 42nd Meeting Division of Fluid Dynamics*. APS Bulletin.

Smith, D. R., Poggie, J. & Smits, A. J. 1990*b* Application of Rayleigh scattering to supersonic turbulent flows. In *Proc. Fifth Int. Symp. on Applications of Laser Techniques to Fluid Mechanics*. Lisbon, Portugal.

Smith, M. W. 1989 Flow visualization in supersonic turbulent boundary layers. Ph.D. thesis, Princeton University, U.S.A.

Smith, M. W., Smits, A. J. & Miles, R. B. 1989 Compressible boundary layer density cross sections by UV Rayleigh scattering. *Optics Lett.* **14**, 916–918.

Smith, R. W. & Smits, A. J. 1991 Effect of Reynolds number on the large structure of turbulent boundary layers. *AIAA Paper* 91-0526.

Smits, A. J., Spina, E. F., Alving, A. E., Smith, R. W., Fernando, E. M. & Donovan, J. F. 1989 A comparison of the turbulence structure of subsonic and supersonic boundary layers. *Phys. Fluids* A **1**, 1865.

Spalart, P. R. 1988 Direct simulation of a turbulent boundary layer up to $Re_\theta = 1410$. *J. Fluid Mech.* **187**, 61–98.

Spina, E. F. 1988 Organized structures in a supersonic turbulent boundary layer, Ph.D. thesis, Princeton University, U.S.A.

Spina, E. F. & Smits, A. J. 1987 Organized structures in a compressible, turbulent boundary layer. *J. Fluid Mech.* **182**, 85–109.

Spina, E. F., Donovan, J. F. & Smits, A. J. 1990 Convection velocity in a supersonic turbulent boundary layer. In *Proc. 12th Symp. on Turbulence*. University of Missouri-Rolla.

Spina, E. F., Donovan, J. F. & Smits, A. J. 1991 On the structure of high-Reynolds-number supersonic turbulent boundary layers. *J. Fluid Mech.* **222**, 293–328.

Walker, J. D. A. 1990 Wall-layer eruptions in turbulent flows. In *Structure of turbulence and drag reduction* (ed. A. Gyr). Springer-Verlag.

Watson, R. D., Harris, J. E. & Anders, J. B. 1973 Measurements in a translational/turbulent Mach 10 boundary layer at high Reynolds number. *AIAA Paper* 73-165.

(a)

(b)

(c)

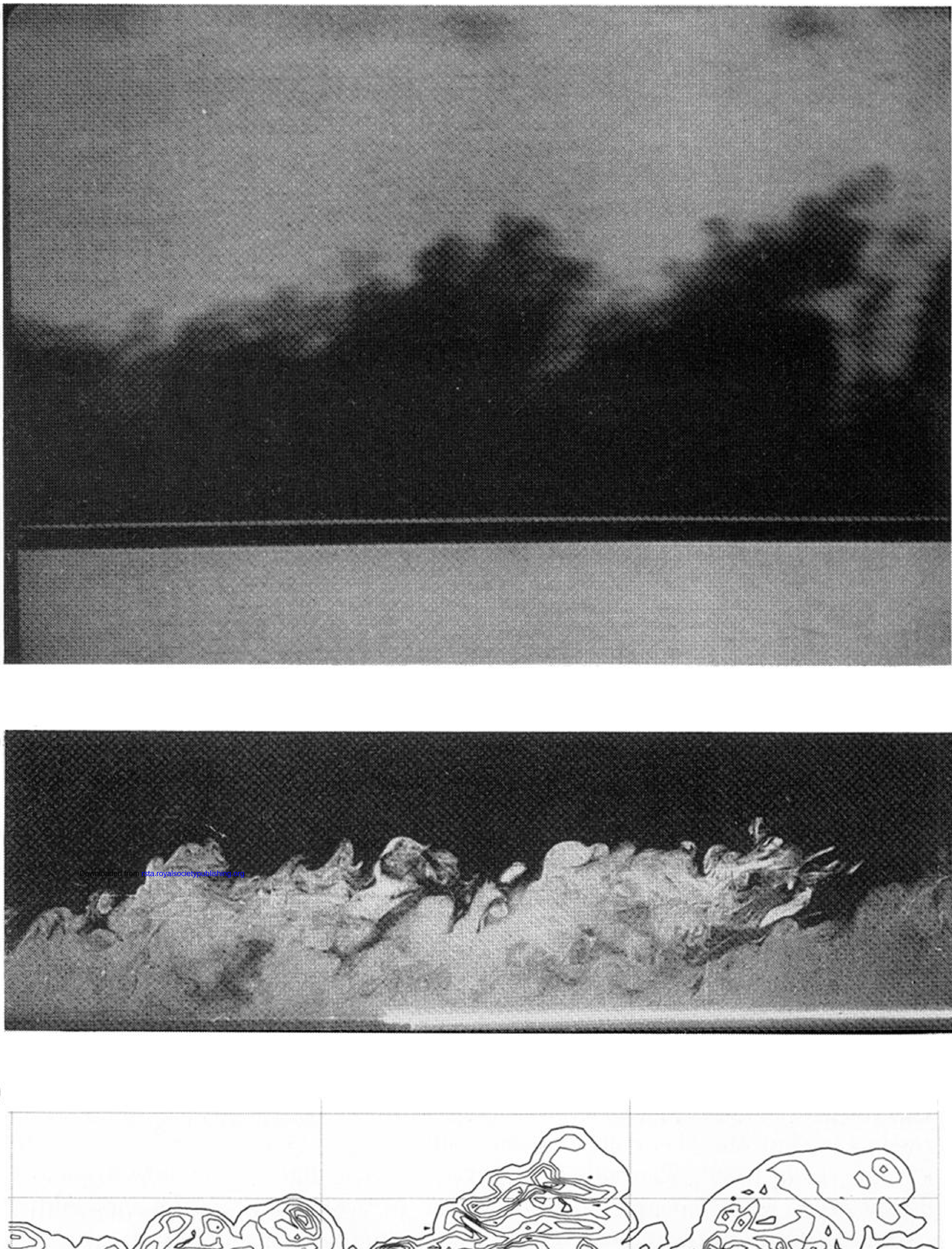

Figure 2. (*a*) Streamwise cross-section of a Mach 2.5 boundary layer with $Re_\theta = 25000$, obtained using Rayleigh scattering; Smith *et al*. (1988). (*b*) Streamwise cross-section of a subsonic boundary layer with $Re_\theta = 4000$, obtained using oil droplet visualization (Falco 1977). (*c*) Streamwise cross-section of a computer-generated subsonic boundary layer with $Re_\theta = 670$, showing iso-vorticity contours. The flow is direct Navier–Stokes simulation (Spalart 1988; Robinson 1990). Figure from Spina *et al*. (1991).

PHILOSOPHICAL TRANSACTIONS OF THE ROYAL SOCIETY A MATHEMATICAL, PHYSICAL & ENGINEERING SCIENCES